Journal of Manufacturing Systems 85 (2026) 473–486

Contents lists available at ScienceDirect

Journal of Manufacturing Systems

journal homepage: www.elsevier.com/locate/jmansys

Technical paper

A double-sided bundle auction mechanism for collaborative additive manufacturing

Mingyue Sun [a], Jinpeng Li [a], Jiaxin Fan [a], Mengdi Zhang [a], Zhiheng Zhao [a,b,*], George Q. Huang [a,b]

[a] Department of Industrial and Systems Engineering, The Hong Kong Polytechnic University, Hong Kong
[b] Research Institute for Advanced Manufacturing, The Hong Kong Polytechnic University, Hong Kong

ARTICLE INFO

Keywords:
Collaborative manufacturing
Additive manufacturing
Resource Exchange
Double-sided auction
Adaptive neighborhood search

ABSTRACT

Collaborative manufacturing has become an essential strategy for improving resource utilization and profitability in the additive manufacturing (AM) industry. In this study, we propose an additive manufacturing collaboration platform (AMCP) to facilitate bilateral resource exchange in decentralized AM environments. To address the challenges posed by the two-way, many-to-many exchange of heterogeneous AM resources in AMCP, we design a five-phase double-sided bundle auction (DBA) mechanism. This mechanism is proven to satisfy incentive compatibility, individual rationality, budget balance, and allocative efficiency, ensuring fair and efficient collaboration among self-interested participants. To optimize the winner determination problem in DBA, which arises from overlapping transactions and flexible bundle bidding, we reformulate it as a maximum weight independent set problem in graph theory. Based on this reformulation, we develop a graph-based adaptive neighborhood search algorithm that balances computational efficiency and solution quality. The experimental results demonstrate that the proposed mechanism is both feasible and robust. It achieves superior social welfare, cooperation rates, and scalability when compared to traditional approaches. Additionally, sensitivity analysis reveals the robustness and resilience of the proposed mechanism, even in the presence of strategic manufacturers.

1. Introduction

With the rapid advancement of additive manufacturing (AM), the technology has become increasingly influential in industrial production, social development, and daily life [1]. The rising demand for highly specialized and intensive AM processing capabilities has highlighted the potential for collaboration among AM manufacturers, particularly in concentrated manufacturing environments [2,3]. Manufacturers frequently encounter scenarios where incoming orders exceed their production capacity or fall beyond their areas of expertise [4,5]. Instead of rejecting such orders, they can collaborate with other manufacturers in the community who possess complementary capabilities by sharing orders. Simultaneously, manufacturers are encouraged to actively seek shared orders from others to maximize the utilization of their own production resources [6–8]. This collaborative AM is facilitated through the two-way exchange of manufacturing orders, enabling decentralized AM manufacturers to adjust their production plans to meet growing demands for personalization.

The challenges of fostering collaboration within a sharing-based AM environment primarily arise from the complexity of two-way overlapping transactions and the involvement of multiple self-interested stakeholders [9]. Unlike centralized or unidirectional distributed resource allocation, which focuses on matching manufacturing resources from a top-down, one-way perspective, collaborative AM systems must account for bilateral resource exchanges [10,11]. In collaborative AM scenario, each AM manufacturer may simultaneously share resources with multiple counterparts while simultaneously requesting resources from others. This transactional overlap, coupled with the departure from traditional one-to-one exchanges to a many-to-many exchange framework, significantly increases the system's complexity. Beyond the inherent challenges of two-way overlapping transactions, the self-interested nature of AM manufacturers further complicates resource exchanges. In contrast to resource allocation scenarios that operate with full and deterministic information,

* Corresponding author at: Department of Industrial and Systems Engineering, The Hong Kong Polytechnic University, Hong Kong.
E-mail address: zhiheng.zhao@polyu.edu.hk (Z. Zhao).

https://doi.org/10.1016/j.jmsy.2026.02.006
Received 23 November 2025; Received in revised form 18 January 2026; Accepted 3 February 2026
Available online 12 February 2026

collaborative AM broker must function with partial and often indistinguishable information shared by autonomous manufacturers [12]. Manufacturers in a two-sided market may strategically misrepresent their preferences or resource capabilities to secure more favorable allocations, which can undermine both the fairness and efficiency of the system [13,14]. Li et al. [15] explore decentralized, negotiation-based coordination mechanisms for smart manufacturing systems and develop a manufacturing resource-based self-organizing scheduling approach to allocate production and logistics tasks through competitive bidding among heterogeneous resource agents. These challenges underscore the necessity of designing a bilateral collaboration mechanism in AM, one that ensures efficient resource exchanges while addressing the strategic behaviors of stakeholders.

The double-sided combinatorial auction is a natural and effective choice for addressing manufacturing resource allocation problems in two-sided markets, as widely demonstrated in prior research [16–19]. In comparison to traditional linear pricing mechanisms commonly used for homogeneous commodities, the collaborative AM resource-sharing problem involves highly heterogeneous and personalized AM orders, where costs are unique to individual manufacturers, and the utility derived from a combination of tasks is often non-additive [20]. These distinct characteristics render traditional double-sided auction mechanisms, such as the McAfee mechanism and its extensions, unsuitable for scenarios involving the exchange of heterogeneous resources [21].

To address the challenges posed by the two-way, many-to-many exchange of heterogeneous AM resources, this study develops an additive manufacturing collaboration platform (AMCP) that leverages a double-sided combinatorial auction mechanism for resource matching and pricing. The primary contributions of this study are summarized as follows:

- An AMCP is designed to provide a structured framework that integrates an auction mechanism to facilitate efficient two-way resource exchanges, thereby establishing the basis for maximizing social welfare.
- A five-phase double-sided bundle auction (DBA) is proposed to effectively manage overlapping transactions and ensures efficient multi-party collaboration. The mechanism ensures key properties, including incentive compatibility, individual rationality, budget balance, and allocation efficiency.
- A graph-based representation is introduced to reformulate the winner determination problem in DBA. Furthermore, a graph-based adaptive neighborhood search (G-ANS) algorithm is developed, employing novel adaptive neighborhood search strategies to identify optimal collaboration.

The remainder of this paper is structured as follows: In Section 2, we review the relevant literature. Section 3 defines the collaborative AM problem in AMCP. The DBA auction mechanism is introduced in Section 4. The algorithmic procedure of G-ANS is explained in Section 5. Section 6 discusses numerical experiments and results. Finally, Section 7 presents the conclusions and outlines directions for future research.

2. Literature review

To provide a comprehensive understanding of the relevant literature, this review organizes the discussion into two aspects: the development of collaborative manufacturing, especially its utilization in AM, and the application of double-sided auction mechanisms for collaborative manufacturing.

2.1. Collaborative manufacturing

Existing research on collaborative manufacturing primarily focuses on its architectural frameworks, aiming to enhance resource sharing, decision-making, and interoperability among distributed manufacturing entities. Guo et al. [22] introduced a cloud–edge collaborative manufacturing framework for AM applications in petroleum equipment manufacturing, identifying key enabling technologies to support such integration. Similarly, Wang et al. [23] extended this perspective by analyzing the production characteristics and collaborative management requirements of multi-workshop discrete manufacturing enterprises, proposing a collaborative manufacturing execution system to optimize coordination. In addition to these architectural developments, recent studies have incorporated mechanism-level innovations into collaborative frameworks. Zheng et al. [9] proposed a blockchain-driven framework for cross-enterprise collaborative manufacturing supply chains, ensuring data credibility and security in distributed environments. Similarly, Zhang et al. [24] examined collaborative manufacturing in mass personalization, proposing an open community collaborative manufacturing framework to enable online resource allocation and matching, thereby improving design efficiency and cost-effectiveness. While these studies provide valuable insights into the design and development of collaborative manufacturing frameworks, they devote comparatively little attention to resource scheduling and allocation methods, which are critical for operational efficiency in collaborative manufacturing.

A key challenge in collaborative manufacturing scheduling arises in distributed multi agents (factories/plants/machines) production planning, where numerous decision variables—such as machine capabilities, resource constraints, and cost optimization—make coordination complex [25,26]. Yuan et al. [27] addressed this by proposing a machine-level collaborative manufacturing architecture, formulating a nonlinear integer optimization model to minimize transportation, production, and sales costs while considering real-world constraints like storage capacity, production substitutions, and order fulfillment rates. Similarly, Cheng et al. [28] proposed a hypernetwork-based scheduling model, incorporating graph coloring algorithms and artificial bee colony optimization to improve task allocation efficiency.

Beyond these optimization and scheduling oriented approaches, recent research has also systematically examined platform-based task assignment in social and collaborative manufacturing environments. For example, Bao et al. [29] review platform-based task assignment for social manufacturing (PBTA4SM) and highlight how digital platforms can match heterogeneous tasks with distributed manufacturing resources. Their survey provides a conceptual and methodological framework for platform-based coordination. While these methods tackle the operational complexity of scheduling and allocation, their integration into collaborative manufacturing platforms remains an open challenge, especially in the context of AM.

While these methods tackle the operational complexity of scheduling and allocation, their integration into collaborative manufacturing platforms remains an open challenge, especially in the context of AM.

Several AM-based collaborative manufacturing platforms, such as 3D Hubs and Shapeways, have already adopted social manufacturing principles, enabling global users to share manufacturing resources [30]. In addition to industrial applications, academic discussions have also explored the integration of collaborative AM platforms. Yoo et al. [31] proposed a social manufacturing ecosystem (SME) to facilitate the realization of manufacturer-driven AM production, particularly in DIY product reconfiguration. However, the inherent complexity of collaborative production increases when multiple self-interested stakeholders participate, each prioritizing individual profitability. Zehetner and Gansterer [7] addressed this perspective by proposed a decentralized collaborative production planning framework for AM, which utilizes a CMfg platform, enabling manufacturers to place bids via a combinatorial second-price reverse auction, aligning individual incentives with overall system efficiency. The integration of AM within such collaborative manufacturing platforms signifies a new wave of industrial transformation, particularly characterized by the emergence of bilateral transactions and cross-interactions among manufacturers, as well as the highly heterogeneous nature of shared resources [32]. However,

existing platform-integrated methods are not well-suited to address these new trends, highlighting the need for more adaptable and efficient mechanisms.

2.2. Double-sided auction for collaborative manufacturing

In collaborative manufacturing, the interplay between multiple stakeholders often complicates efficient resource allocation [33]. This environment naturally evolves into a two-sided market, where multiple buyers (demand-side) and sellers (supply-side) simultaneously bid for resources. The double-sided auction mechanism is particularly well-suited for this environment, as it ensures optimal resources matching while maintaining market equilibrium [34]. Notably, McAfee [35] demonstrated that double auction can achieve pareto efficiency in multi-agent environments, making it a viable solution for manufacturing resource allocation in collaborative manufacturing.

While few studies explicitly address the application of double-sided auctions within collaborative AM systems, existing research in cloud manufacturing and distributed manufacturing offers valuable insights into how such mechanisms can handle resource allocation challenges. For instance, Kang et al. [2] explored a cloud manufacturing framework designed to mitigate temporary shortages in manufacturing resources by enabling enterprises to share capacities. Their study introduced two multi-unit double auction mechanisms to allocate manufacturing cloud services at equilibrium trade prices. In the context of AM, De Antón et al. [36] proposed an iterative combinatorial double auction for e-platform-based transactions of AM subcomponents, aiming to maximize social welfare while incorporating privacy-preserving strategies. Similarly, Chen et al. [37] developed a peer-to-peer production capacity matching model, leveraging blockchain-based transparency and an iterative double auction mechanism to determine optimal pricing and quantity allocation while safeguarding participants' private information. These studies demonstrate the potential of double-sided auction mechanisms in addressing resource allocation challenges, particularly in distributed manufacturing settings. However, most of this research assumes relatively straightforward production constraints and homogeneous transaction environments, limiting its applicability to more complex and decentralized systems.

To address the challenges of collaborative manufacturing under complex production constraints and self-interested behaviors, Liu et al. [38] introduced a strategic double auction framework where resource demanders and providers bidding dynamically based on budget constraints, delivery time, reservation prices, and expected profits. Their mechanism ensures economic incentives are preserved, even in markets with incomplete information. Similarly, Cheng et al. [39] proposed a novel supply-demand matching model for shared manufacturing resources, integrating double auction-based supply-demand matching with multi-attribute negotiation to refine transaction details. In decentralized manufacturing environments, self-interested agents further complicate collaborative scheduling. Liu et al. [6] examined the multi-agent parallel machine scheduling problem, where consumer agents and resource agents prioritize their own profit maximization. Since these agents operate under private information constraints, centralized scheduling models become infeasible. To address this, an iterative combinatorial auction mechanism was designed, enabling collaborative scheduling without compromising data privacy. Building on these insights, rethinking auction designs is essential to address the unique characteristics, particularly within the context of additive manufacturing.

3. Problem description and formulation

3.1. Problem description

Consider an AMCP operating within a loosely structured AM alliance, where multiple self-interested and autonomous AM manufacturers coexist. Each manufacturer manages its own orders and aims to maximize its individual utility. Due to mismatched capabilities or resource constraints, manufacturers strategically distribute surplus orders and select combined orders from others to optimize their profits. Collaboration among AM manufacturers is facilitated by the AMCP, which functions as a third-party auctioneer. Through the efficient exchange and reallocation of orders enabled by the AMCP, participating manufacturers are guaranteed a utility level no lower than what they would achieve without collaboration. This ensures that all participants have sufficient incentives to engage in the collaborative process. A comparison of manufacturers' performance before and after collaboration via the AMCP is presented in Fig. 1.

Let M denote the set of manufacturers. A manufacturer in this context acts as both buyers (i.e., AM service purchaser) and sellers (i.e., AM service provider). Let M^b denote manufacturers acting as buyers and M^s represent seller. In our collaborative setting, when acting as a buyer, a manufacturer posts orders and is willing to pay for having them processed. For each order, the buyer specifies the maximum amount it is willing to pay, which we model as its valuation for that order. When acting as a seller, a manufacturer offers its available capacity to process orders submitted by others. In this role, it submits bids that specify the required compensation for processing certain individual orders or bundles of orders. Note that a manufacturer may simultaneously belong to both $M^b$and M^s if it submits orders as a buyer and offers capacity as a seller.

For a buyer $m \in M^b$, manufacturers outsource production orders to other manufacturers. The set of sharing orders for each buyer $m \in M^b$ is denoted as $R^b_m = \{r^b_{m,k} | k \in k^m\}$, where$k^m$ is the index set of all sharing orders of buyer m. Each order $r^b_{m,k}$ is associated with a bidding price $b^b_{m,k}$, based on the true cost $v^b_{m,k}$. The complete set of sharing orders offered by all buyers is denoted as $R = \{\sum_{m \in M^b} R^b_m\}$.

For a seller $m \in M^s$, manufacturers bid on combination of sharing orders offered by other buyers to form profitable bundles. Each seller $m \in M^s$ submits a set of bids, denoted as $C^s_m = \cup\{c^s_{m,n}, n \in N\}$, where N is the set of all combinations being auctioned, and each bundle n contains one or more orders. For a given bundle n, the bid price submitted by seller m is $b^s_{m,n}$, determined based on the true cost $v^s_{m,n}$. We assume that each seller can win at most one bundle. This assumption reflects the practical constraint that sellers place bids only on bundles that are attractive to them. If the combination of two or more orders within a bundle is more profitable than handling them separately, sellers submit a higher bid for the combined bundle.

3.2. Problem formulation

Our goal is to maximize the social welfare through optimizing the matching decision for manufacturers. In standard welfare economics and mechanism design, social welfare in is defined as the sum of agents' utilities in a given mechanism [40]. In line with it, social welfare in our setting is defined as the total utility of all participating agents in the AMCP environment, including manufacturers M, as well the auctioneer AMCP.

The utility of a manufacturer $m \in M$ is determined by the net balance between the payment received from the platform for providing AM services and the cost incurred from outsourcing external orders. The AMCP's utility is the difference between the total payments collected from buyers and the total expenditure distributed to sellers. Adding up the two groups' utilities, the payment received by M and the expenditure term of AMCP can be cancelled out, such that the social welfare equals the real values of all accepted buyers less the costs of all winning sellers. If all agents bid truthfully, the optimal matching can be solved from the following social welfare maximization problem, denoted as $W(M, AMCP)$:

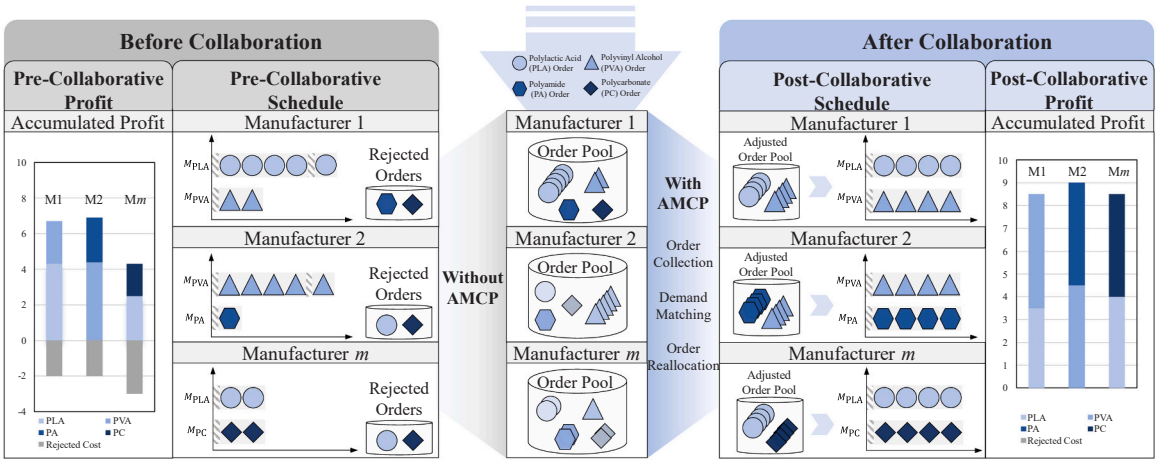

Fig. 1. Comparison before and after collaborative processing.

$$\max W(M,\quad AMCP) = \sum_{m\in M^b}\sum_{k\in R_m^b} b_m^b \alpha(r_{m,k}^b) - \sum_{m\in M^s}\sum_{n\in N} b_{m,n}^s \beta\left(c_{m,n}^s\right) \tag{1}$$

s.t.

$$\sum_{n\in N}\beta\left(c_{m,n}^s\right) \le 1,\quad \forall m \in M^s, \tag{2}$$

$$\sum_{m\in M^s}\sum_{n\in N, r\in n} \delta_n^r \beta\left(c_{m,n}^s\right) = \alpha(r_{m,k}^b),\quad \forall r \in R_m^b, \forall k \in k^m \tag{3}$$

$$\beta\left(c_{m,n}^s\right) = \{0,\quad 1\}, \forall n \in N, \forall m \in M^s, \tag{4}$$

$$\alpha(r_{m,k}^b) = \{0,\quad 1\}, \forall m \in M^b,\quad \forall k \in k^m \tag{5}$$

where $\alpha(r_{m,k}^b)$ denotes whether buyer $m \in M^b$ trades in the efficient allocation, and $\beta\left(c_{m,n}^s\right)$ denotes whether the bid of seller $m \in M^s$, $c_{m,n}^s$, is selected. The objective of $W(M, AMCP)$ is to find an efficient allocation that maximizes social welfare. Constraints (2) ensure that each seller can win at most one of their submitted bids. Constraints (3) ensure the supply-and-demand balance for each request, while implicitly guaranteeing that each order can be allocated to at most one seller. It is worth noting that the indicator variable δ_n^r is used to specify whether a particular order is included in a given bundle. The composition of orders within a bundle n is deterministic at the time of seller bidding, meaning that δ_n^r is predetermined and known. Constraints (4) define the binary nature of the decision variables for sellers' bids. Constraints (5) define the binary nature of the decision variables for buyers' bids.

4. DBA auction mechanism

In this section, we propose a five-phase DBA auction mechanism designed specifically for the AMCP. The goal of the DBA is to efficiently coordinate order sharing among dual-role manufacturers while keeping the interaction with the platform friendly for participants.

Compared with conventional single-sided or single-item auctions, and with monolithic auction mechanisms, the proposed DBA is tailored to several distinctive features of collaborative AM in the AMCP. On the one hand, it supports many-to-many transactions over overlapping bundles of heterogeneous orders, which cannot be handled effectively by simple one-to-one or single-item auctions. On the other hand, the DBA framework explicitly separates the responsibilities of dual-role manufacturers and the platform. Manufacturers only need to submit sharing orders and place XOR bundle bids according to their preferences, while the AMCP is responsible for constructing the order pool, solving the combinatorial allocation problem, and computing payments. This design reduces both the strategic and computational burden on participants.

4.1. Auction procedure

The proposed five-phase procedure for the DBA mechanism is inspired by the logistics collaboration framework outlined by Gansterer [41]. The DBA mechanism is designed to be participant-friendly, allowing for the free combination of orders, thereby reducing unnecessary computational complexity during bidding. The DBA auction for the AMCP operates as follows, with Fig. 2 illustrating how the mechanism facilitates collaboration among manufacturers.

- **Order sharing:** Each manufacturer selects and offers multiple production orders to the AMCP, specifying their minimum acceptable price.
- **Order collection:** The AMCP compiles a shared pool of orders and provides freely combinable bundles of orders.
- **Bundle bidding:** Each manufacturer submits an XOR bid, specifying all their preferred bundles along with the corresponding bid values.
- **Winner determination:** The AMCP reallocates orders among manufacturers according to their bids to maximize the total social welfare of the coalition.
- **Payment calculation:** Payments are calculated by the AMCP.

4.2. Payment calculation

Here, we focus on payment calculation, which plays a central role in ensuring that manufacturers have no incentive to misreport their valuations. Our design is inspired by the classical Vickrey–Clarke–Groves (VCG) mechanism. In a standard VCG mechanism, the payment of each participant is set equal to the externality that this participant imposes on all other participants, that is, the difference between the total welfare of the others when this participant is absent and when it is present. As a result, each participant's utility coincides with its marginal contribution to the total social welfare [35–37].

Following the same principle as the classical VCG mechanism while being applied to a bundle-based, dual-role setting, we design a VCG-inspired method to compute the payments for dual-role manufacturers in our bundle-based sharing market. The payment for manufacturer m, denoted as p_m, is calculated as $p_m = v_m - (W(M) - W(M\backslash m))$, where v_m is manufacturer m's total valuation, $W(M)$ represents the total social welfare with all agents, and $W(M\backslash m)$ is the social welfare excluding manufacturer m. the total valuation v_m is determined by $v_m = \sum_{k\in R_m^b} v_{m,k}^b - v_{m,n}^s$, where $\sum_{k\in R_m^b} v_{m,k}^b$ is the valuation of its bids as a buyer,

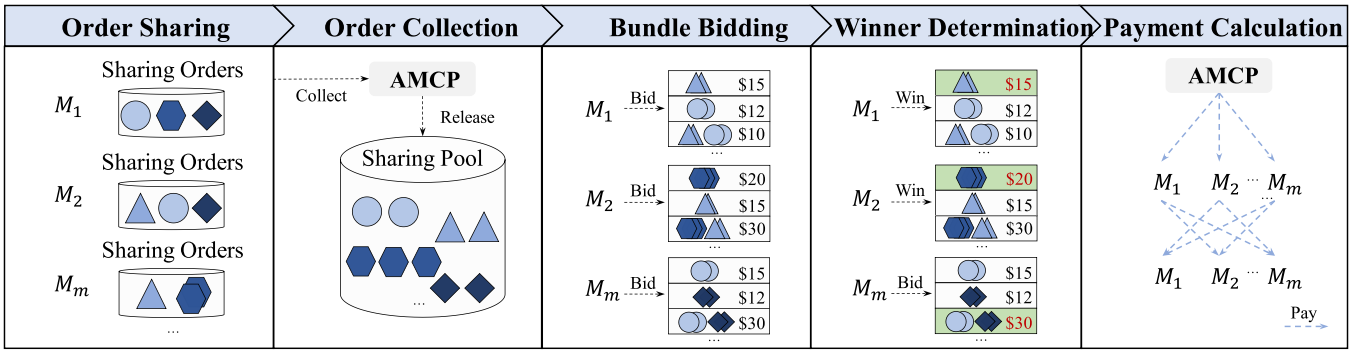

Fig. 2. Five-phase auction framework.

and $v^s_{m,n}$ denotes its ask valuation as a seller. It is worth noting that, under truthful bidding, the submitted bid values $b^b_{m,k}$ and $b^s_{m,n}$ are equal to their respective true valuations $v^b_{m,k}$ and $v^s_{m,n}$. Another important metric for auction participant m is utility u_m, which is defined as the difference between its true valuation and payment: $u_m = v_m - p_m$. Substituting the expression for $p_m$into the utility definition yields $u_m = W(M) - W(M\backslash m)$, which shows that the utility of manufacturer $m$equals its marginal contribution to the total social welfare.

Dual-role manufacturers may exhibit a synergy effect, where integrated participation as both buyer and seller can yield different utility compared to single-role manufacturers. To demonstrate this, consider a market with three dual-role manufacturers M_1, M_2, and M_3, who act as service buyers and share orders A, B, and C, priced at 6, 7, and 8, respectively. The posted prices represent the maximum amounts that manufacturers are willing to pay to have their requests fulfilled. Therefore, they can be interpreted as the buyers' valuations. After the orders are announced, all manufacturers act as service sellers by submitting bids for serving individual orders or bundles of orders. Table 1 presents the bids for all possible bundles.

In the efficient allocation of this example, M_1 is assigned the bundle [B&C] based on its bid of 12, and M_2 is assigned order [A] based on its bid of 6.

So, the total payment to the service sellers is 12 +6 = 18 and the total valuation of the three posted orders is 6 + 7 + 8 =21. Hence, the social welfare in this example is defined as the total valuation of the completed orders minus the total payment to the service sellers, that is, $W(M) = 21 - 18 = 3$.

However, significant differences arise between the single-role and dual-role cases. Take M_1 as an example.

In the single-role case, Suppose that M_1 is treated separately as a pure buyer and as a pure seller.

(i) As a buyer, we only consider M_1's role in demanding a sharing order. When buyer M_1 is excluded, orders A is excluded. In optimal allocation, M_1 service bundle [B&C] with 12, and the total valuation of the completed orders B and C is 7 + 8 = 15. So, social welfare of $W(M\backslash M^b_1)$= 15–12 = 3, Therefore, M_1's utility as a buyer is $u^b_1 = W(M) - W(M\backslash M^b_1) = 3 - 3 = 0$.

(ii) As a seller, we only consider M_1's role in providing service capacity. When seller M_1 is excluded, the remaining manufacturers can still serve all three orders. In this case, the efficient allocation is that M_3 provides bundle [A&B&C] with a bid of 19, so the total payment to service sellers is 19, and the total valuation of the three orders remains 21. Hence, the social welfare becomes $W(M\backslash M^s_1) = 21 - 19 = 2$. Accordingly, M_1's utility as a seller is $u^s_1 = W(M) - W(M\backslash M^s_1) = 3 - 2 = 1$.

Table 1
Bundle bidding price.

Bundle	[A]	[B]	[C]	[A&B]	[B&C]	[A&C]	[A&B&C]
M_1	6	7	7	13	12	13	19
M_2	6	7	8	14	14	13	20
M_3	7	7	8	13	15	16	19

If M_1 participates only as a buyer and only as a seller in two separate single-role markets, its total utility is $u^b_1 + u^s_1 = 0 + 1 = 1$.

Dual-role case. In contrast, when M_1 is allowed to participate as a dual-role manufacturer (both as a buyer and as a seller) in a single integrated market.

If dual-role manufacturer M_1 is excluded entirely, the remaining manufacturers can still serve orders B and C jointly. In this case, the efficient allocation is that M_2 provides bundle [B&C] with a bid of 14. The total valuation of the completed orders is then 7 + 8 = 15, and the total payment to the sellers is 14, so $W(M\backslash M_1) = 15 - 14 = 1$. Therefore, the utility of dual-role M_1 is $u_1 = W(M) - W(M\backslash M_1) = 3 - 1 = 2$.

Comparing the two situations, M_1's total utility is 1 in the separated single-role markets, but increases to 2 in the integrated dual-role market. This highlights a synergy effect, where simultaneous participation as both buyer and seller may increase a manufacturer's overall utility compared to participating only in separate single-role markets.

4.3. Properties

In this section, we propose and prove the properties of the DBA mechanism, including truthful reporting, allocative efficiency, individual rationality, and weak budget balance (under the submodularity of the social welfare function $W(M)$. The detailed proofs are as follows:

Theorem 1. Truthful bidding is an ex-post Nash equilibrium in the DBA auction.

Proof. It suffices to prove the theorem under the condition of $u_m > 0$, which is equal to $v_m - p_m$. If seller m ($m \in M$) bids truthfully in terms of his valuation function v^b_m and $v^s_{m,n}$, he receives a VCG payment, $p^s_{m,n} = v_m - (W(M) - W(M\backslash m))$. Suppose that agents in $M\backslash m$ bid truthfully. When manufacturer m bids $\hat{b}^b_{m,k}$ and ask $\hat{b}^s_{m,n}$. Also, let M' be the set of winners if manufacturer m submits $\hat{b}^b_{m,k}$ and $\hat{b}^s_{m,n}$. Let M^* denote the set of winning manufacturers in the auction.

If truthful reporting is not a dominant strategy for seller m, then

$$\hat{u}_m > u_m \Leftrightarrow v_m - \hat{p}_m > v_m - p_m \Leftrightarrow W(M') - W(M\backslash m) > W(M^*) - W(M\backslash m) \Leftrightarrow W(M') > W(M^*)$$

This contradicts the efficiency property of $W(M^*)$, which ensures that no alternative allocation can achieve a higher social welfare. So, truthful reporting is the dominant strategy for manufacturer m.■

Theorem 2. The DBA auction is allocatively efficiency and individually rational.

Proof. (*Allocative Efficiency*) According to the objective of max$W(M, AMSP)$, the DBA auction maximizes the total social welfare. Theorem 1 states that the manufacturers bid truthfully to maximize their individual utility. Hence, the DBA auction maximizes social welfare given truthful bids from all the agents.

(*Individual Rationality*) Participants will always have non-negative utility by participating in the auction. That is, no participant ends up worse off by joining the auction compared to not participating.

From the VCG payment rule, it follows that $p_m = v_m - (W(M) - W(M\backslash m))$. We can achieve $p_m \le v_m$, since $W(M) \ge W(M\backslash m)$, $m \in M$. In this context, seller $m \in M$ always get a non-negative utility $u_m = v_m - p_m \ge 0$. So, sellers in the auction are individual rational.∎

Definition 1. The value function $W(M)$ is submodular if, for any subcoalition $S \subseteq M$ and any participant m, it satisfies:

$$W(S) - W(S\backslash m) \ge W(M) - W(M\backslash m),$$

i.e., the marginal contribution of a participant m to a smaller coalition S is at least as large as their marginal contribution to the grand coalition M.

Theorem 3. When the social welfare function $W(M)$ is submodular, the auction can achieve weak budget balance, i.e., $u_p \ge 0$.

Proof. If we apply the VCG payment, the total platform utility is given by:

$$\begin{aligned} u_p &= \sum_{m\in M^*} p_m = \sum_{m\in M^*} (v_m - (W(M) - W(M\backslash m))) \\ &= \sum_{m\in M^*} \left(b^b_m - b^s_{m,n} - (W(M) - W(M\backslash m)) \right) \\ &= W(M^*) - \sum_{m\in M^*} (W(M) - W(M\backslash m)). \end{aligned}$$

From **Definition 1**, we know:

$$W(m) - W(\varnothing) \ge W(M) - W(M\backslash m),$$

which, when summed over all $m \in M^*$, implies:

$$\sum_{m\in M^*} (W(m) - W(\varnothing)) \ge \sum_{m\in M^*} (W(M) - W(M\backslash m)).$$

Substituting this result into the expression for u_p, we obtain:

$$u_p \ge \sum_{m\in M^*} W(m) - \sum_{m\in M^*} (W(M) - W(M\backslash m)) \ge 0.$$

Thus, the auction satisfies weak budget balance when the social welfare function $W(M)$ is submodular. ∎

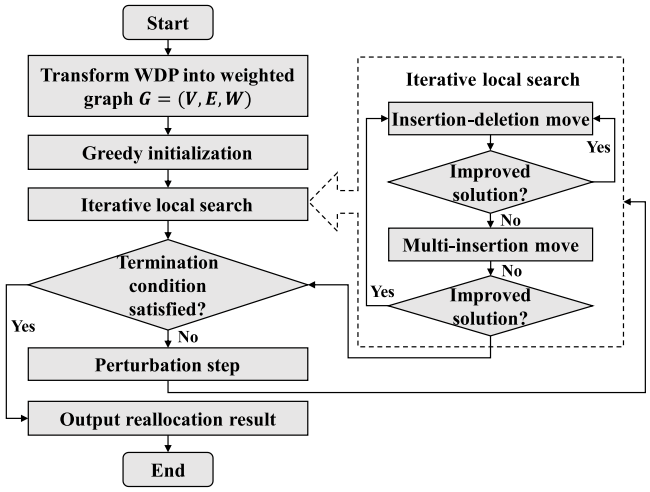

Fig. 3. Overall workflow of the proposed G-ANS algorithm.

5. Graph-based adaptive neighborhood search algorithm

To solve this reformulated maximum weight independent set problem, we propose a novel algorithm named graph-based adaptive neighborhood search (G-ANS), which exploits the graph representation to efficiently determine the winning bundles. The overall framework of G-ANS consists of three main components: (1) a graph construction step; (2) a greedy initialization procedure; (3) an iterated local search (ILS) algorithm [42] and (4) an adaptive acceptance mechanism.

In the graph construction step, the auction information is transformed into a weighted graph representation. So that the winner determination problem is reformulated as finding a maximum weight independent set in this graph. The details of this transformation are provided in Section 5.1. Based on this graph, the greedy initialization procedure then constructs a feasible reallocation that serves as the starting solution for the subsequent search. The detailed greedy initialization process is presented in Section 5.2. Finally, the ILS component iteratively improves the current solution in order to approximate the maximum weight independent set under the given auction information. Within this ILS procedure, we design two problem-specific neighborhood moves and an jointly designed adaptive acceptance rule. These ILS components are described in detail in Section 5.3, while the adaptive acceptance mechanism of G-ANS is further elaborated in Section 5.4.

The overall workflow of G-ANS is illustrated in Fig. 3, and the corresponding pseudo-code is given in Algorithm 1.

Algorithm 1. Procedure of the G-ANS

Input: Order set R, bundle set B^s_m by $m \in M^s$
Output: Set of matched bundle-order pairs, total social welfare
1: 1: Convert bundle set B^s_m into graph $G = (V, E, W)$
2: $S_0 = \text{GreedyInitialize}(G)$
3: $S^* = S_0$
4: $iter = 1$
5: **While** $iter \le max\_iter$ **do**
6: $S' = \text{ILS}(S, G)$
7: $S^* = \text{Acceptance}(S', S^*)$, $iter = iter + 1$
8: **End While**
9: **Return** S^*

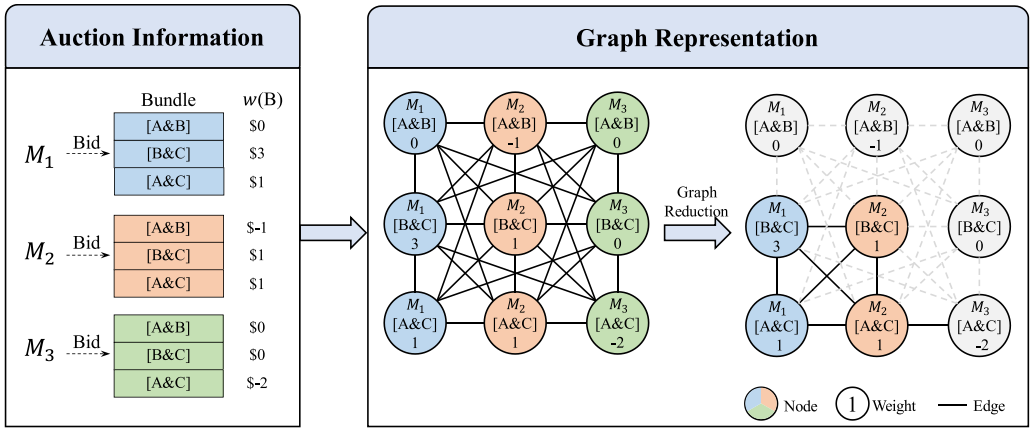

Fig. 4. Graph representation of bundle-based auction information.

The following sections provide a detailed explanation of the greedy initialization heuristic, enhancement moves in ILS process and the design of the adaptive acceptance mechanism.

5.1. Graph representation of the bundle-based Auction

In this section, we illustrate the core idea of representing the solution space on a graph. The winner determination problem $W(M.AMCP)$aims to identify a set of winning bundles that maximizes social welfare. Equivalently, the task is to select an optimal combination of non-overlapping bundles that yields the highest social welfare. To this end, we reformulate the problem as a weighted graph model and convert the search from finding a set of non-overlapping bundles to finding a weighted independent set of vertices. In graph-theoretic terms, the problem can be cast as a maximum weight independent set (MWIS) problem.

In the reformulation, each bundle B is represented as a vertex $v \in V$ in the graph. The weight $w(B)$ of vertex v is defined as the marginal value of bundle B, that is, the total sharing cost of the orders in B minus the seller's minimum bid price for B. An edge $e \in E$ is introduced between two vertices if their corresponding bundles share at least one order or if they are submitted by the same manufacturer, as required by the XOR bidding constraints. Thus, all bundles submitted by the same manufacturer are mutually connected. Under this construction, any independent set of vertices corresponds to a feasible allocation of non-overlapping bundles that satisfies the XOR constraints, and the total weight of the independent set corresponds to the resulting social welfare.

This transformation allows the auction winner determination problem to be modeled as a weighted graph $G = (V, E, W)$. Fig. 4 illustrates this process. We select a subset of representative bundles from the example in Section 4.2. Manufacturers submit bids on bundles, and the AMCP first computes the marginal value $w(B)$ for each bundle B. These bundles are then mapped to vertices according to the above principles. Subsequently, we apply a reduction step that removes all vertices with non-positive weight $w(B) \leq 0$. This graph reduction eliminates dominated or non-profitable bundles and thus accelerates the subsequent search for the maximum weight independent set.

5.2. Greedy initialization procedure

To construct an initial feasible solution to the MWIS formulation, we adopt a simple yet effective greedy procedure. Let $G = (V, E, W)$ denote the graph, where each vertex $v \in V$ corresponds to a bundle and is associated with weight $w \geq 0$. The procedure maintains a candidate vertex set $A \subseteq V$ and an independent set S.

At each step, we select a vertex from A with the largest weight w. The selected vertex v is added to the independent set S, and both v and all its neighbors $N(v)$ are removed from the candidate set A. This process is repeated until A becomes empty. The resulting independent set S is used as the starting solution for the subsequent local search. The resulting independent set provides a feasible solution with relatively high total weight, which is then used as the initial solution for the subsequent local search phase.

5.3. Enhancement moves in ILS

To improve the performance of the ILS, we propose two enhancement moves: the insertion-deletion move and the multi-insertion move. The design of the two enhancement moves is closely tailored to the structure of the graph arising from the bundle-based auction. The detailed procedure for these moves is outlined in Algorithm 2 below.

Algorithm 2. ILS with two enhancement moves

Input: Graph $G = (v, e, w)$, Current independent set solution $S \in V$
Output: Improved independent set solution S^*
Initialize neighborhood index $k \leftarrow 1$
$S^* \leftarrow S$
While $k \leq 2$ **do**
  If $k = 1$ **then** // Insertion-deletion move
    Randomly select a vertex $v \in V \backslash S^*$
    Remove all neighbor vertex set $N(v) \cap S^*$
    Add v to S^*
    Insert additional free vertices to restore maximality
  Else if $k = 2$ **then** // Multi-insertion move
    Randomly select a vertex $u \in S^*$
    Remove u from S^*
    Identify a pair of non-adjacent vertices $v_1, v_2 \in V \backslash S^*$ such that $v_1, v_2 \notin N(w)$ for all $w \in S^*$
    Addv_1, v_2 to S^*
    Insert additional free vertices to restore maximality
  End If
  If weight(S^*)>weight(S) **then**
    $S \leftarrow S^*, k \leftarrow 1$
  Else
    $k \leftarrow k + 1$
  End If
End While
Return S^*

In the insertion-deletion move, a single vertex is added to the current solution while a randomly selected subset of its adjacent vertices is simultaneously removed to maintain independence. Afterward, additional vertices are inserted as needed to restore the solution's maximality while ensuring it remains an independent set. This is particularly relevant in our setting, where choosing one high-value bundle may require discarding several overlapping bundles that cover the same requests.

In the multi-insertion move, one vertex is removed from the solution, and two new vertices are inserted to expand the search space more effectively. Subsequently, the solution is examined to determine whether any additional free vertices can be incorporated without violating the independence constraint. In the auction context, a single selected bundle may block the inclusion of several smaller but jointly more beneficial bundles. By removing such a blocking bundle and inserting two non-adjacent bundles that are compatible with the remaining solution, the move can capture cases where one medium-weight bundle is replaced by two disjoint bundles with higher combined weight.

Fig. 5 provides a schematic illustration of these enhancement moves on a small subgraph of the auction instance.

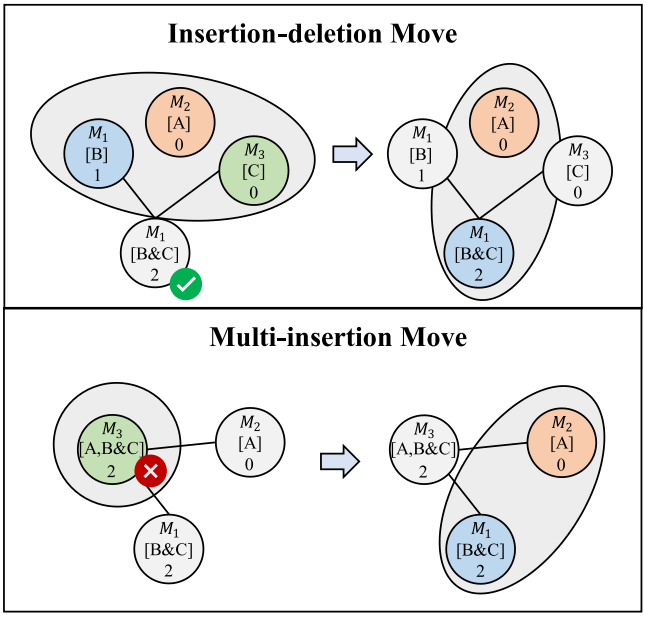

Fig. 5. Example of problem-specific enhancement moves.

5.4. Adaptive acceptance mechanism in G-ANS

This subsection describes the adaptive acceptance mechanism used in G-ANS, which decides whether a newly obtained local optimum is accepted as the current solution. Instead of using a classic Metropolis-type random acceptance rule, G-ANS employs an adaptive counter k to

regulate the trade-off between intensification and diversification. When the search frequently finds better solutions, the counter k is frequently reset or reduced, so that the algorithm tends to accept mainly improving moves, thereby reinforcing intensification. Conversely, when the search stagnates and no improvement is observed for a long period, k gradually increases and eventually exceeds a threshold, which in turn triggers stronger perturbations and a higher willingness to accept inferior solutions, enhancing diversification.

Fig. 6 illustrates the overall workflow of this mechanism.

To further improve performance, we incorporate a perturbation adaptive mechanism to dynamically balance intensification (exploiting high-quality solutions) and diversification (exploring new regions of the solution space). The perturbation strength is controlled by a parameter ρ, which determines the magnitude of changes applied to the current solution. The specific value of ρ is not fixed a priori but is calibrated through a parameter sensitivity analysis described in Section 6.2.

To prevent premature convergence and escape local optima, we design an adaptive acceptance mechanism. This mechanism is governed by the acceptance flexibility parameter σ, which controls the tolerance for accepting inferior solutions. A candidate solution is always accepted if it improves the current solution S. Otherwise, inferior solutions may be accepted with a probability. Additionally, a local counter mechanism resets whenever an improved solution is found, ensuring a flexible and adaptive search process. Similar to ρ, the value of σ is tuned empirically in Section 6.2 based on its impact on solution quality and robustness.

The detailed procedure is outlined in Algorithm 3 below.

Algorithm 3. Procedure of perturbation and adaptive acceptance mechanism

Input: Current independent set solution S, best-so-far solution S^*, maximum iterations without improvement c_{max}, perturbation strength parameter ρ
Output: Updated solution S, updated best solution S^*

Initialize local counter $i \leftarrow 0$, perturbation counter $k \leftarrow 1$
Initialize best solution weight $w^* \leftarrow \text{weight}(S^*)$, local best $w \leftarrow \text{weight}(S^*)$
While stopping criterion not met **do**
  Generate perturbed solution $S' \leftarrow$Perturb(S)
  Apply local search: $S' \leftarrow$LocalSearch(S′), reset $k \leftarrow 1$
  $\Delta \leftarrow$weight(S')>weight(S)
  If $\Delta > 0$ **then**
    $S^* \leftarrow S'$, $w^* \leftarrow \text{weight}(S')$, k $\leftarrow 1$//Intensification: always accept improvement
  Else
    $P \leftarrow P(\text{size}(S)*\sigma)$
    draw $u \sim Uniform(0,1)$
    If $u < P$ **then**
      $S^* \leftarrow S'$, $k \leftarrow 1$
    Else
      $w \leftarrow$weight(S), $k \leftarrow k -$size(S)/ρ
    End If
  End If
  If weight(S)>weight(S^*)
      $S^* \leftarrow S'$, $w \leftarrow$ weight(S), Reset $k \leftarrow 1$
  Else
    $k \leftarrow k + 1$
  End If
Return S^*

6. Numerical experiments

In this section, we assess the performance of the proposed auction mechanism through a series of numerical experiments.

First, we fine-tune the parameters of G-ANS to validate its effectiveness. Then, we conduct a sensitivity analysis of the proposed DBA mechanism, demonstrating its truthfulness even in scalable environments. This analysis also provides valuable insights into two key evaluation metrics from the administrator's perspective: social welfare and cooperation rate.

6.1. Experimental setup

To evaluate the proposed mechanism, we simulate a distinct market scenario where manufacturers can submit multiple orders and bid on preferred bundles, reflecting the characteristics of a real-world market. All numerical experiments are conducted on a personal computer equipped with an Intel i5-13600KF processor (4.95 GHz), 64 GB of RAM, and an NVIDIA GeForce RTX 3060 Ti GPU.

The bidding prices for individual orders are generated from a normal distribution with a mean of 100 and a variance of 20. Similarly, the asking prices for bundles are drawn from a normal distribution, where the mean depends on the number of orders in the bundle (n^r) and is calculated as $n^r(100 - 10n^r)$, with a variance of 20. This pricing model is designed to simulate economies of scale. The maximum number of orders per bundle is limited by each manufacturer's production capacity, which is indirectly represented by the number of orders they submit.

The bidding prices for individual orders are generated from a normal

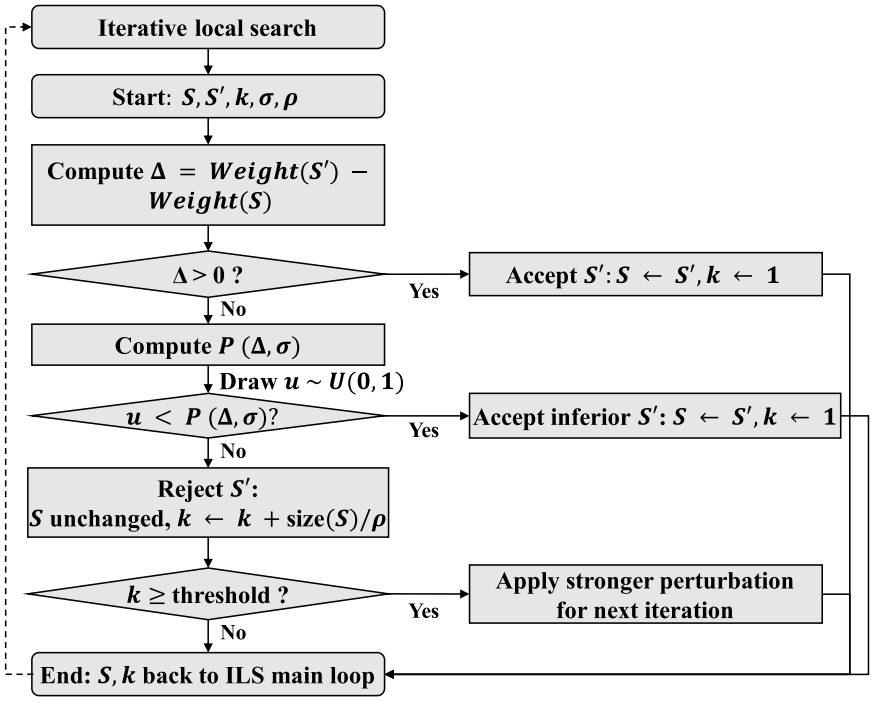

Fig. 6. Overall workflow of adaptive acceptance mechanism.

distribution with a mean of 100 and a variance of 20. These values are chosen to produce price levels and dispersion that are consistent with the relative cost structure assumed in our experimental setting, ensuring that both buyers' valuations and sellers' costs lead to economically meaningful trades (i.e., neither trivially always-profitable nor almost never-profitable). We have also verified that moderate perturbations of these parameters within a reasonable range do not change the qualitative comparison among the tested mechanisms and algorithms.

6.2. Parameter tuning

In this section, we report results from parameter tuning on perturbation strength parameter ρ and the acceptance flexibility parameter σ, which from our experience, are very important to the algorithm. To minimize computational costs, we employ a selective tuning strategy rather than exhaustively testing all possible parameter combinations across all instance sizes.

We conduct a two-stage parameter tuning procedure for ρ and σ. In the first stage, we evaluate eight candidate values of ρ and σ in the range [0.01,10] on a subset of benchmark instances and identify three promising values (ρ=0.05,0.5,1.0, σ=0.05,0.1,0.5) that yield relatively better performance. In the second stage, we perform a joint experiment on these ρ values and several candidate σ values to examine their interaction and to determine the best parameter combination. The final settings of ρ and σ used in all subsequent experiments correspond to the combination that achieves the best trade-off between solution quality, stability, and runtime.

The tuning process begins with an initial test to identify the three best-performing values for ρ and σ which are then used for further tuning on larger instance sizes. In the initial test, we evaluate instances with 100 manufacturers, each submitting up to 10 sharing orders and 20 bundles, with a maximum of 10 orders per bundle. The G-ANS algorithm runs for 4000 iterations for each parameter setting. The detailed results of this parameter sensitivity analysis are summarized in Fig. 7 and Fig. 8.

The results in Fig. 7 and Fig. 8 show the G-ANS's ability to gradually improve and converge under almost all parameter configurations. For most ρ values, the algorithm's performance improves steadily and converges to a stable objective value within 4000 iterations. Initially, $\rho = 1$ performs similarly to other values, but after 800 iterations, it improves sharply and significantly outperforms the others, indicating that $\rho = 1$ achieves the best balance between exploration and exploitation. In contrast, $\rho = 0.01$ exhibits a non-monotonic trend with occasional

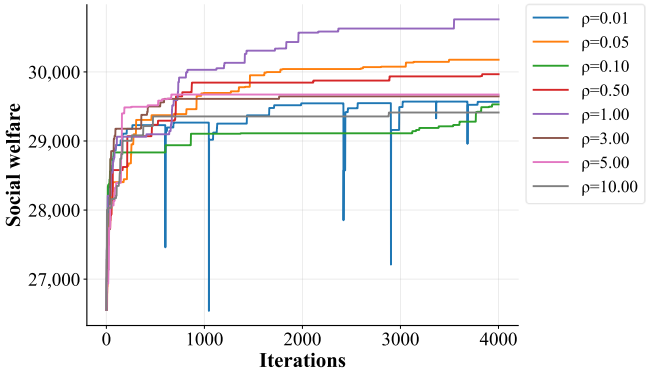

Fig. 7. Tuning of range of perturbation strength parameter ρ.

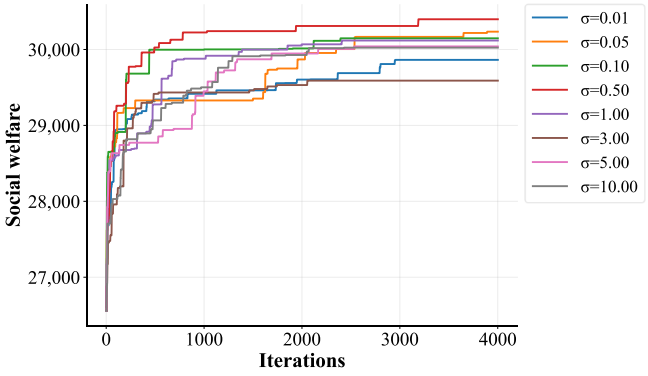

Fig. 8. Tuning of range of acceptance flexibility parameter σ.

decreases in objective value. This behavior is attributed to minimal perturbation, which increases the likelihood of getting trapped in local optima and hinders consistent improvement.

Compared to ρ, the influence of σ on convergence is more subtle but still observable. The algorithm converges steadily across all σ values, demonstrating robustness and relative insensitivity to parameter variations. However, σ values less than 1 (e.g., 0.5, 0.1) tend to produce higher objective values by maintaining a balanced acceptance of inferior solutions, effectively escaping local optima without compromising solution quality.

Based on the analysis of the two parameters, the top-performing values for ρ and σ were identified as ρ = 1,0.05, and 0.5 and σ = 0.5,0.05, and 0.1. These combinations resulted in a total of 9 parameter configurations, as shown in Table 3.

These parameter combinations were further evaluated on three large-scale instances (L1, L2, and L3) to assess their performance under different instance sizes. The specific characteristics of each instance are summarized in Table 4.

To evaluate the performance of the parameter combinations under different instance sizes, we generated 10 test cases for each instance size and computed the average objective value. Given the significant variations in absolute social welfare values across different instance sizes, direct comparisons were not feasible. To address this, we normalized the social welfare values within each instance size. Specifically, the worst-performing result was normalized to 0, and the best-performing result was normalized to 1, ensuring a fair comparison across scales. The normalized results are presented in Fig. 9. From Fig. 9, we observe that combination 6 ($\rho = 0.05,\ \sigma = 0.1$) consistently achieved the highest normalized social welfare across both small and large instance groups. This indicates its superior performance in balancing exploration and exploitation, regardless of the problem size.

To further identify a parameter setting with robust performance across all problem sizes, we averaged the normalized results for each combination over the three instance sizes (L1, L2, and L3). The aggregated performance is depicted in Fig. 10. As shown in Fig. 10, combination 6 ($\rho = 0.05,\ \sigma = 0.1$) demonstrated the most significant advantage, with the highest average normalized social welfare (0.921) among all parameter combinations. This consistent performance across multiple scales highlights its robustness and adaptability to varying problem complexities. Based on these findings, we selected combination 6 as the optimal parameter configuration for subsequent experiments.

6.3. Comparison of gurobi and G-ANS

To evaluate the performance of the proposed G-ANS algorithm, we compared it with the Gurobi solver across different problem scales using two primary metrics: social welfare and cooperation rate. Social welfare, when no commission is charged by the AMCP, equals the aggregate utility of all manufacturers; collaboration rate is the proportion of successfully fulfilled orders among all submitted orders. Experiments were conducted with 100, 200, and 300 manufacturers, each with corresponding sharing orders of 10, 20, and 30, and maximum production capacities.

For each problem size, 10 independent runs were performed, and the average results are summarized in Table 5. Gurobi was given a time limit of 600 s per run. Notably, for instances with 400 manufacturers, Gurobi was unable to find a feasible solution within the time limit. As shown in Table 5, the G-ANS algorithm demonstrates clear advantages over Gurobi in terms of social welfare, cooperation rate, and computational efficiency, particularly as the problem size increases. For smaller instances with 100 manufacturers, G-ANS achieves social welfare results very close to those of Gurobi. However, as the problem size grows, G-ANS outperforms Gurobi, with a 0.27 % improvement for 200 manufacturers and a 4.59 % improvement for 300 manufacturers, showing its ability to maintain high solution quality and even deliver better results for larger problems.

The cooperation rates achieved by both methods are comparable across all scenarios. While G-ANS performs slightly lower than Gurobi for 100 manufacturers, it surpasses Gurobi for larger instances, achieving 30.31 % for 200 manufacturers and 25.65 % for 300 manufacturers, compared to Gurobi's 29.53 % and 23.54 %, respectively. This indicates that G-ANS can sustain cooperation rates effectively as the problem complexity increases.

In terms of computational efficiency, G-ANS consistently outperforms Gurobi. For all tested instances, Gurobi requires significantly more time, often exceeding 600 s when the number of manufacturers is greater than 100. Notably, for instances with 400 manufacturers, Gurobi fails to find a feasible solution within the time limit. In contrast, G-ANS maintains high efficiency, solving even the largest instance in just 230.27 s, which is over 60 % faster than Gurobi. This robustness in computation time demonstrates the scalability and practicality of G-ANS for larger and more complex problems.

Overall, the computational results show that the proposed G-ANS algorithm is well suited to the bundle-based sharing problem considered in this work. Compared with the benchmark methods, G-ANS consistently delivers higher social welfare and makes better use of manufacturing capacities, particularly on large-scale instances with many overlapping bundles and dual-role manufacturers. These results indicate that the specific design of G-ANS, including graph representation, graph-based neighborhood moves and adaptive acceptance mechanism, aligns well with both the combinatorial structure of the problem and the practical constraints of the manufacturing marketplace.

6.4. Sensitivity analysis of DBA

In this section, we conduct a sensitivity analysis of the DBA mechanism from three perspectives: (1) the proportion of untruthful manufacturers; (2) scenarios with abundant processing capacity, where supply exceeds demand; and (3) scenarios representing a thriving market, where demand exceeds supply. For consistency, we consider three large-scale instances, with the specific settings detailed in Table 4.

6.4.1. Sensitivity analysis of the proportion of untruthful manufacturers

To assess the impact of strategic misreporting, we evaluate how different proportions of untruthful manufacturers (0 %, 10 %, and 50 %) affect social welfare and cooperation rate. For each instance size, 10 random instances are generated, and the results are visualized in Fig. 11 and Fig. 12. Fig. 11 illustrates the distribution of social welfare across scenarios and untruthful proportions. It is evident that social welfare declines as the proportion of untruthful manufacturers

Table 4
Instance size settings of instances (L1, L2, and L3).

Instance	Manufacturer	Sharing Orders	Bundles	Containing Orders
L1	100	10	20	10
L2	150	15	30	15
L3	200	20	40	20

Table 3
Parameter combinations of ρ and σ used for algorithm tuning.

Combinations	P1	P2	P3	P4	P5	P6	P7	P8	P9
ρ	1	1	1	0.05	0.05	0.05	0.5	0.5	0.5
σ	0.5	0.05	0.1	0.5	0.05	0.1	0.5	0.05	0.1

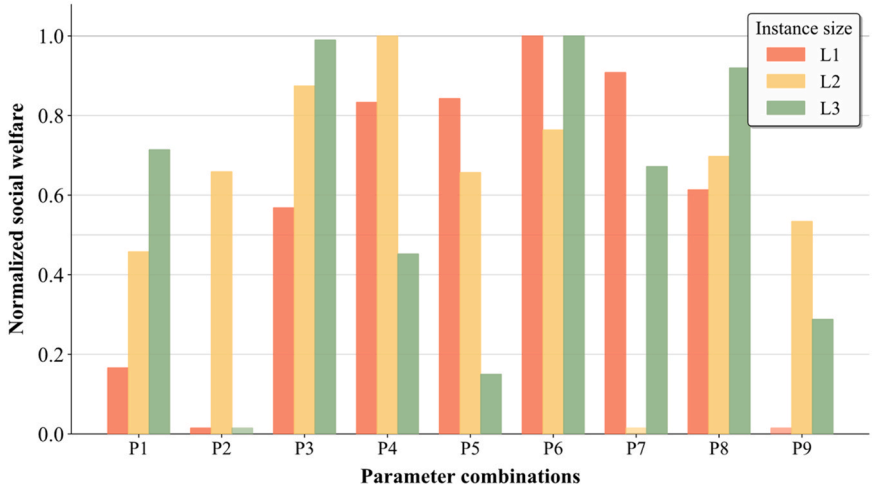

Fig. 9. Comparison of normalized social welfare.

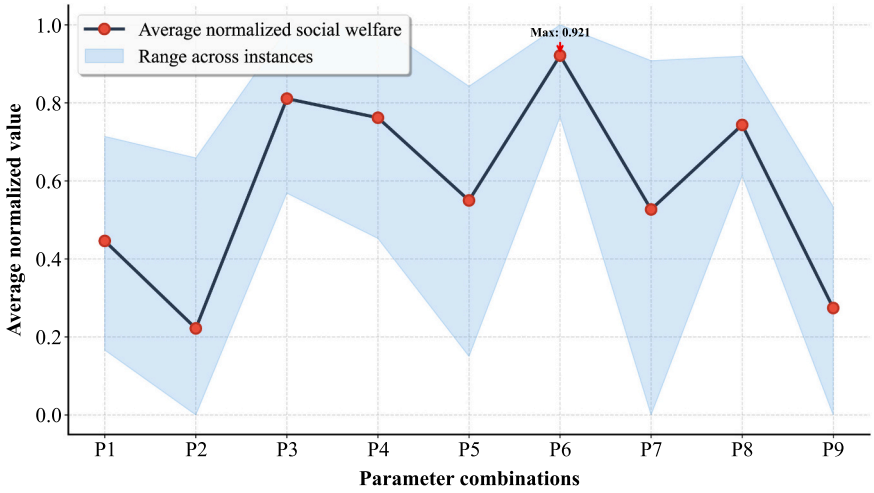

Fig. 10. Average normalized social welfare for each parameter combination.

Table 5
Comparison of Gurobi and G-ANS performance across different problem scales.

M	Gurobi			G-ANS		
	Social Welfare	Cooperation Rate	Time (s)	Social Welfare	Cooperation Rate	Time (s)
100	10672.49	38.10 %	68.61	9971.19	36.08 %	2.82
200	31337.24	29.53 %	645.12	31420.61	30.31 %	92.91
300	54603.74	23.54 %	651.10	57108.2	25.65 %	230.27

increases, regardless of the instance size. In each scenario, the highest social welfare is achieved when all manufacturers are truthful. As the proportion of untruthful manufacturers increases to 10 % and then 50 %, there is a notable reduction in social welfare. This pattern demonstrates the detrimental effect of dishonest behavior on overall market efficiency. Additionally, the absolute value of social welfare increases with the instance size, as expected, but the negative impact of untruthfulness is observed consistently across all scales. For instance, in the largest instance group (L3), social welfare drops sharply from its peak at 0 % untruthful manufacturers to a significantly lower value when 50 % of manufacturers are untruthful.

Fig. 12 shows the corresponding cooperation rates. These scenarios, denoted as L1, L2, and L3, represent different market scales and complexities. Fig. 12 illustrates a similar trend for the cooperation rate. As the proportion of untruthful manufacturers increases, the cooperation rate consistently decreases for each scenario. When all manufacturers are truthful, the market achieves the highest level of cooperation, suggesting that truthfulness fosters greater collaboration among participants. However, as untruthfulness rises, the willingness or ability of manufacturers to cooperate diminishes, leading to reduced market connectivity and efficiency. This decline is particularly pronounced in larger instances, where the cooperation rate not only decreases but also becomes more dispersed. This suggests that larger and more complex markets are even more sensitive to the effects of strategic misreporting.

6.4.2. *Sensitivity analysis of varying supply and demand*

In this section, we investigate the impact of varying supply and demand on social welfare and cooperation rate. We consider a setting with 200 manufacturers, each submitting 10 bundles. By adjusting the number of sharing orders and the production capacity (i.e., the

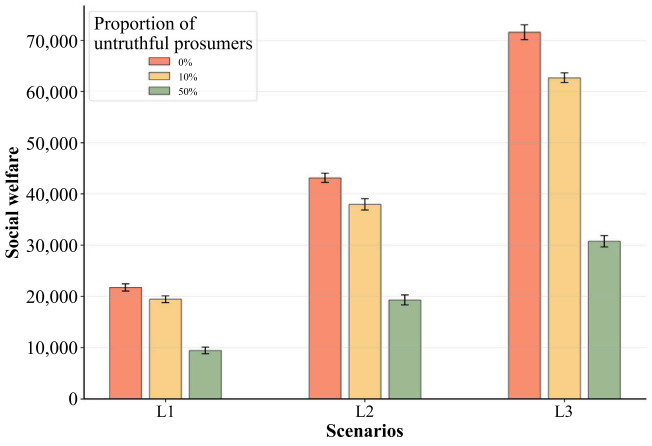

Fig. 11. Social welfare across scenarios and proportion of untruthful manufacturers.

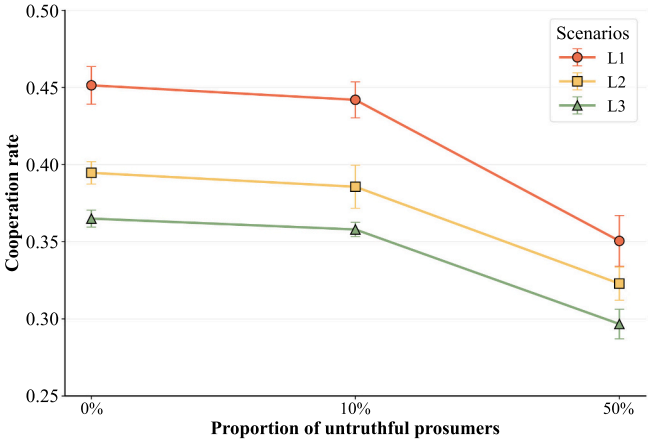

Fig. 12. Cooperation rate across scenarios and proportion of untruthful manufacturers.

maximum number of orders contained in a single bundle), we create a spectrum of market conditions ranging from a buyer-dominated market to a seller-dominated market.

Six distinct supply-demand scenarios are considered to represent different supply-demand scenarios. For instance, Scenario (1, 20) represents a buyer's market, where each manufacturer submits one sharing order and the maximum shared production capacity is 20. For each scenario, 10 random instances are generated, with results shown in Fig. 13: orange dots represent social welfare, and green crosses denote the cooperation rate. Fig. 13 reveals several important trends regarding the interplay between supply and demand in the market. As the scenario transitions from a buyer market to a seller market, social welfare initially increases, reaching a peak at intermediate scenarios, and then begins to decline. This suggests that social welfare is maximized when supply and demand are relatively balanced, likely due to more efficient resource allocation and greater matching opportunities.

In contrast, the cooperation rate exhibits a monotonically decreasing trend as the market shifts toward excess demand. In scenarios with abundant supply, the cooperation rate is highest, indicating that a greater proportion of manufacturers are able to engage in cooperative transactions. As the market becomes increasingly demand-driven, the cooperation rate drops significantly, implying that intensified competition for limited resources hampers the ability of manufacturers to collaborate.

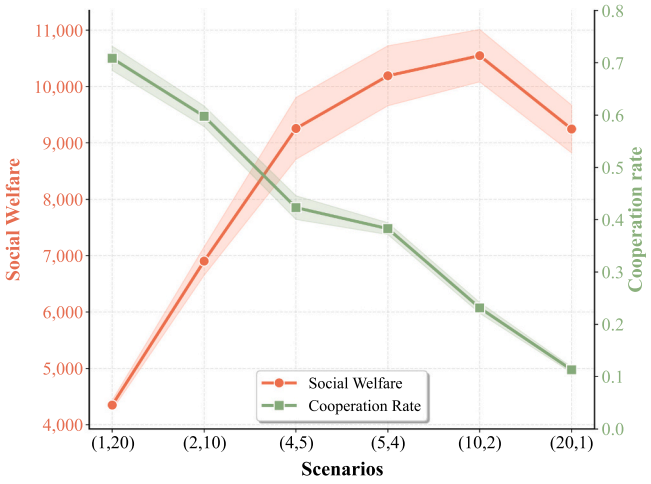

Fig. 13. Social welfare and cooperation rate across supply-demand scenarios.

These findings suggest that if the AMCP intends to charge entry fees or commissions from transactions, it would be optimal to target markets where social welfare is maximized. In contrast, if the goal is to enhance the cooperation rate, the decision should be based on the overall market environment.

7. Conclusion

To increase machine utilization and the profitability of AM service, many AM manufacturers have begun experimenting with collaborative manufacturing platforms. This paper proposes a DBA framework to address the matching and pricing challenges inherent in collaborative requirements within AMCP environments. In the proposed mechanism, a manufacturer simultaneously shares resources with multiple parties while outsourcing its own needs, effectively managing overlapping transactions. The DBA mechanism ensures incentive compatibility, individual rationality, budget balance, and allocation efficiency. To address the computational complexity of overlapping transactions and heterogeneous resources, we developed an efficient G-ANS algorithm. This algorithm models complex resource dependencies and incorporates an adaptive neighborhood search strategy to achieve optimal resource allocation. It ensures computational tractability while attaining allocative efficiency.

Our computational study demonstrates the practical feasibility and robustness of the proposed mechanism, even in the presence of strategic manufacturers. Sensitivity analysis further evaluates its performance under several operational factors: (1) the proportion of untruthful manufacturers, (2) scenarios where supply exceeds demand, and (3) scenarios where demand exceeds supply. Results show that the G-ANS algorithm outperforms Gurobi in social welfare, cooperation rate, and computational efficiency, particularly in larger problem sizes. Social welfare and cooperation rates decline as the proportion of untruthful manufacturers increases, highlighting the importance of truthful participation. Additionally, social welfare peaks when supply and demand are balanced, while cooperation rates are highest in supply-abundant markets, providing insights into optimizing AMCP operations under varying market conditions.

The proposed auction mechanisms are adaptable to other exchange environments. While the current model assumes fixed manufacturer orders, an important extension would be to incorporate order uncertainty using probabilistic or stochastic modeling. However, achieving incentive-compatible, budget-balanced auctions under such conditions remains a significant challenge.

CRediT authorship contribution statement

Mingyue Sun: Writing – original draft, Validation, Software, Methodology, Conceptualization. **George Q. Huang:** Investigation, Funding acquisition, Conceptualization. **Zhiheng Zhao:** Supervision, Investigation, Funding acquisition, Conceptualization. **Mengdi Zhang:** Supervision, Methodology, Investigation, Conceptualization. **Jiaxin Fan:** Writing – original draft, Validation, Methodology. **Jinpeng Li:** Validation, Resources, Methodology.

Declaration of Competing Interest

The authors declare that they have no known competing financial interests or personal relationships that could have appeared to influence the work reported in this paper.

Acknowledgments

The authors would like to express their sincere thanks to the financial support from the Hong Kong Research Grants Council (No. PolyU15203025, T32-707/22-N, C7076-22GF), National Natural Science Foundation of China (No. 52305557), Guangdong Basic and Applied Basic Research Foundation (No. 2024A1515011930, 2025A1515012669), Research Institute for Advanced Manufacturing (RIAM) of The Hong Kong Polytechnic University (No. CDLU, CDLM, CDJX).

References

[1] Gibson I, Rosen D, Stucker B, Khorasani M. Additive Manufacturing Technologies. Cham: Springer International Publishing; 2021. https://doi.org/10.1007/978-3-030-56127-7.
[2] Kang K, Xu SX, Zhong RY, Tan BQ, Huang GQ. DoublE Auction-based Manufacturing Cloud Service Allocation in an Industrial Park. IEEE Trans Autom Sci Eng 2022;19:295–307. https://doi.org/10.1109/TASE.2020.3029081.
[3] Sunley P, Evenhuis E, Harris J, Harris R, Martin R, Pike A. Renewing industrial regions? Advanced manufacturing and industrial policy in Britain. Reg Stud 2023;57:1126–40. https://doi.org/10.1080/00343404.2021.1983163.
[4] Gu X, Koren Y. Mass-Individualisation – the twenty first century manufacturing paradigm. Int J Prod Res 2022;60:7572–87. https://doi.org/10.1080/00207543.2021.2013565.
[5] Yang M, Li C, Tang Y, Wu W, Zhang X. A collaborative resequencing approach enabled by multi-core PREA for a multi-stage automotive flow shop. Expert Syst Appl 2024;237:121825. https://doi.org/10.1016/j.eswa.2023.121825.
[6] Liu Y, Sun S, Wang XV, Wang L. An iterative combinatorial auction mechanism for multi-agent parallel machine scheduling. Int J Prod Res 2022;60:361–80. https://doi.org/10.1080/00207543.2021.1950938.
[7] Zehetner D, Gansterer M. Decentralised collaborative job reassignments in additive manufacturing. Int J Prod Res 2023:1–19. https://doi.org/10.1080/00207543.2023.2285403.
[8] Chen J, Ye X, Xie N, Sang Y-W, Sterna M. Benders decompositions for order acceptance and scheduling in additive manufacturing. Eur J Oper Res 2025:S0377221725008069. https://doi.org/10.1016/j.ejor.2025.10.005.
[9] Zheng K, Ding K, Hui J, Zhang F, Lv J, Chan FTS. Blockchain-based credible manufacturing data sharing for a collaborative manufacturing supply chain. Int J Prod Res 2024;62:2233–54. https://doi.org/10.1080/00207543.2023.2217292.
[10] Xue X, Wang S, Zhang L, Feng Z. Evaluating of dynamic service matching strategy for social manufacturing in cloud environment. Future Gener Comput Syst 2019;91:311–26. https://doi.org/10.1016/j.future.2018.08.028.
[11] Zhang Y, Tang D, Zhu H, Li S, Nie Q. A flexible configuration method of distributed manufacturing resources in the context of social manufacturing. Comput Ind 2021;132:103511. https://doi.org/10.1016/j.compind.2021.103511.
[12] Sueur C, Deneubourg J-L, Petit O. From Social Network (Centralized vs. Decentralized) to Collective Decision-Making (Unshared vs. Shared Consensus). PLOS ONE 2012;7:e32566. https://doi.org/10.1371/journal.pone.0032566.
[13] Gansterer M, Hartl RF, Vetschera R. The cost of incentive compatibility in auction-based mechanisms for carrier collaboration. Networks 2019;73:490–514. https://doi.org/10.1002/net.21828.
[14] Ding X, Qi Q, Jian S. Truthful online double auctions for on-demand integrated ride-sourcing platforms. Eur J Oper Res 2023. https://doi.org/10.1016/j.ejor.2023.12.004.
[15] Li Y, Liu Q, Li X, Gao L. Manufacturing resource-based self-organizing scheduling using multi-agent system and deep reinforcement learning. J Manuf Syst 2025;79:179–98. https://doi.org/10.1016/j.jmsy.2025.01.004.
[16] Zhou H, Wu T, Chen X, He S, Guo D, Wu J. Reverse Auction-Based Computation Offloading and Resource Allocation in Mobile Cloud-Edge Computing. IEEE Trans Mob Comput 2023;22:6144–59. https://doi.org/10.1109/TMC.2022.3189050.
[17] Li Z, Jiang C, Kuang L. Double Auction Mechanism for Resource Allocation in Satellite MEC. IEEE Trans Cogn Commun Netw 2021;7:1112–25. https://doi.org/10.1109/TCCN.2021.3087173.
[18] Kang K, Zhong RY, Xu SX, Tan BQ, Wang L, Peng T. Auction-based cloud service allocation and sharing for logistics product service system. J Clean Prod 2021;278:123881. https://doi.org/10.1016/j.jclepro.2020.123881.
[19] Liu Y, Sun S, Shen G, Wang XV, Wang L. Designing a double auction mechanism for parallel machines scheduling with multiple consumer agents and resource agents. Expert Syst Appl 2025;268:126275. https://doi.org/10.1016/j.eswa.2024.126275.
[20] Fowler JW, Mönch L. A survey of scheduling with parallel batch (p-batch) processing. Eur J Oper Res 2022;298:1–24. https://doi.org/10.1016/j.ejor.2021.06.012.
[21] Xu SX, Huang GQ, Cheng M. Truthful, Budget-Balanced Bundle Double Auctions for Carrier Collaboration. Transp Sci 2017;51:1365–86. https://doi.org/10.1287/trsc.2016.0694.
[22] Guo L, He Y, Wan C, Li Y, Luo L. From cloud manufacturing to cloud–edge collaborative manufacturing. Robot ComputIntegr Manuf 2024;90:102790. https://doi.org/10.1016/j.rcim.2024.102790.
[23] Wang H, Liu L, Fei Y, Liu T. A collaborative manufacturing execution system oriented to discrete manufacturing enterprises. Concurr Eng 2016;24:330–43. https://doi.org/10.1177/1063293X16640591.
[24] Zhang X, Ming X, Bao Y. Online merchant resource allocation and matching for open community collaborative manufacturing (OCCM) in mass personalization model. Adv Eng Inform 2023;55:101872. https://doi.org/10.1016/j.aei.2022.101872.
[25] Kang K, Qing Tan B, Zhong RY. Multi-attribute negotiation mechanism for manufacturing service allocation in smart manufacturing. Adv Eng Inform 2022;51:101523. https://doi.org/10.1016/j.aei.2021.101523.
[26] Fu Y, Hou Y, Wang Z, Wu X, Gao K, Wang L. Distributed scheduling problems in intelligent manufacturing systems. Tsinghua Sci Technol 2021;26:625–45. https://doi.org/10.26599/TST.2021.9010009.
[27] Yuan H, Hu Q, Bi J, Gong G, Zhang J, Zhou M. Machine-Level Collaborative Manufacturing and Scheduling for Heterogeneous Plants. IEEE Internet Things J 2024;11:16591–603. https://doi.org/10.1109/JIOT.2024.3354251.
[28] Cheng Y, Bi L, Tao F, Ji P. Hypernetwork-based manufacturing service scheduling for distributed and collaborative manufacturing operations towards smart manufacturing. J Intell Manuf 2020;31:1707–20. https://doi.org/10.1007/s10845-018-1417-8.
[29] Bao Y, Ming X, Zhang X, Tao F, Leng J, Liu Y. Platform-based task assignment for social manufacturing (PBTA4SM): State-of-the-art review and future directions. J Manuf Syst 2025;78:328–50. https://doi.org/10.1016/j.jmsy.2024.12.007.
[30] Naghshineh B. Additive manufacturing technology adoption for supply chain agility: a systematic search and review. Int J Prod Res 2024:1–33. https://doi.org/10.1080/00207543.2024.2356629.
[31] Yoo B, Ko H, Chun S. Prosumption perspectives on additive manufacturing: reconfiguration of consumer products with 3D printing. Rapid Prototyp J 2016;22:691–705. https://doi.org/10.1108/RPJ-01-2015-0004.
[32] Jiang P, Leng J, Ding K. Social manufacturing: a survey of the state-of-the-art and future challenges. 2016 IEEE Int Conf Serv Oper Logist Inform (SOLI) 2016:12–7. https://doi.org/10.1109/SOLI.2016.7551654.
[33] Tao F, Zhang Y, Cheng Y, Ren J, Wang D, Qi Q, et al. Digital twin and blockchain enhanced smart manufacturing service collaboration and management. J Manuf Syst 2022;62:903–14. https://doi.org/10.1016/j.jmsy.2020.11.008.
[34] Ren S, Liang C, Liu Y, Wang J, Wang C. Evolutionary game-based warehousing resources sharing strategy for logistics industry under product-service system paradigm. Adv Eng Inform 2025;67:103560. https://doi.org/10.1016/j.aei.2025.103560.
[35] McAfee RP. A dominant strategy double auction. J Econ Theory 1992;56:434–50. https://doi.org/10.1016/0022-0531(92)90091-U.
[36] De Antón J, Villafáñez F, Poza D, López-Paredes A. An iterative price-based combinatorial double auction for additive manufacturing markets. Comput Ind Eng 2024;197:110602. https://doi.org/10.1016/j.cie.2024.110602.
[37] Chen Y, Lin F, Chen Z, Tang C, Chen C. Optimal production capacity matching for blockchain-enabled manufacturing collaboration with the iterative double auction method. IEEE/CAA J Autom Sin 2024:1–13. https://doi.org/10.1109/JAS.2024.124626.
[38] Liu ZH, Wang ZJ, Yang C. Multi-objective resource optimization scheduling based on iterative double auction in cloud manufacturing. Adv Manuf 2019;7:374–88. https://doi.org/10.1007/s40436-019-00281-2.
[39] Cheng Y, Yu C, Xu S, Zhao S. A novel supply-demand matching model for shared manufacturing resources. Int J Comput Integr Manuf 2024:1–25. https://doi.org/10.1080/0951192X.2024.2426152.
[40] Krishna V. Auction theory. Academic press; 2009.
[41] Gansterer M, Hartl RF, Sörensen K. Pushing frontiers in auction-based transport collaborations. Omega 2020;94:102042. https://doi.org/10.1016/j.omega.2019.01.011.
[42] Nogueira B, Pinheiro RGS, Subramanian A. A hybrid iterated local search heuristic for the maximum weight independent set problem. Optim Lett 2018;12:567–83. https://doi.org/10.1007/s11590-017-1128-7.